

Atomic Nature of Organometallic-Vapor-Phase-Epitaxial Growth

P. H. Fuoss, D. W. Kisker, G. Renaud, and K. L. Tokuda

AT&T Bell Laboratories, Holmdel, New Jersey 07733

S. Brennan and J. L. Kahn

Stanford Synchrotron Radiation Laboratory, Stanford, California 94309

(Received 18 May 1989)

In situ x-ray scattering has been used to study a growing film (ZnSe on GaAs) during organometallic-vapor-phase epitaxy. This first *in situ* study of non-ultrahigh-vacuum growth revealed a surprisingly stable and well-ordered $p(2 \times 1)$ reconstruction during growth despite the presence of organic reaction by-products. Also, dramatic changes in the specular x-ray reflectivity were found while investigating transient kinetic effects during alternate-source epitaxy. These results demonstrate the power of *in situ* x-ray-scattering studies in the characterization of these complex processes.

PACS numbers: 68.55.Ce, 61.10.Lx, 61.50.Cj, 81.15.Gh

Despite the immense scientific and technological importance of chemical-vapor-phase deposition (CVD), little is known about the detailed atomistic mechanisms by which it occurs.¹ This lack of knowledge is contrasted with molecular-beam epitaxy (MBE) where a close, symbiotic relationship has existed between the development of growth techniques and the development of surface-sensitive structural probes. In particular, the surface structures present on the surface before and during MBE growth have been studied using low-energy electron diffraction and reflection high-energy electron diffraction (RHEED). In return, development of these techniques has been spurred by the importance of understanding growth mechanisms and their relationship to the growth of high-quality materials.

The situation for non-UHV techniques, such as organometallic-vapor-phase epitaxy (OMVPE), is much different because electron-based probes cannot be utilized. While a number of other probes such as mass spectrometry,² infrared spectroscopy,³ and reflectance-difference spectroscopy⁴ have been used to study the phenomenology of CVD processes, much remains to be learned about the detailed atomic mechanisms. For example, the growth of ZnSe can occur by the following reaction:



where Et represents an ethyl radical. However, this apparently simple reaction must occur via a sequence of at least three steps. First, there are chemical reactions which can occur in the vapor phase (e.g., decomposition of the organometallics). Second, chemical reactions and diffusion must occur on the surface of the growing material. Finally, structural changes must be induced in the overlayer to affect the transformation between surface and bulk structures.

In this paper, we describe the first *in situ* x-ray measurements which explore the atomic mechanisms and kinetics associated with OMVPE growth. Using the ex-

tremely bright x radiation from an undulator on the PEP storage ring, we have made real-time measurements of the initial stages of epitaxial growth of ZnSe on GaAs (001) surfaces. In the following, we describe our experimental approach and results including the surprising discovery of an extremely sharp $p(2 \times 1)$ reconstruction on the growing ZnSe and measurements of the kinetically limited response of the surface to chemical transients.

The measurements described in this paper have been made using the grazing-incidence x-ray scattering geometry^{5,6} and a diffractometer operated in the z -axis configuration.⁷ This geometry offers several advantages for x-ray diffraction from surfaces. However, for the experiments described here the necessity to control convective currents in the reactor is the most compelling reason to use the z -axis geometry. If a conventional four-circle geometry were used, the surface would change orientation during scans of diffracted intensity perpendicular to the surface, changing the convective flow patterns. The associated growth fluctuations would make quantitative interpretation of the data very difficult.

Difficulties associated with achieving uniform growth also strongly affect the choice of a synchrotron-radiation source. Typical high-resolution synchrotron diffraction experiments use a vertical scattering plane because the vertical source divergence is 25–50 times smaller than the horizontal divergence. For CVD growth, a vertical scattering plane would result in nonuniform growth. Our experiments took advantage of the exceptional collimation (100 μrad horizontally and 86 μrad vertically) of undulator radiation from the PEP storage ring at the Stanford Synchrotron Radiation Laboratory (SSRL) by using a horizontal scattering plane to avoid this nonuniform growth. At a photon energy of 9500 eV (just below the Zn K absorption edge), the PEP undulator produced 2.5×10^{10} photons/sec into a $0.1 \times 1.5\text{-mm}^2$ entrance slit.

The experiments described here were performed in a specially designed OMVPE reactor and gas-handling system.⁸ This reactor was used to grow ZnSe films on

GaAs substrates which had a resistivity of $> 10^7 \Omega \text{ cm}$ and which were oriented to within 0.1° of the (001) direction. The ZnSe films were deposited from Et_2Zn and Et_2Se sources which were transported to the reactor by 99.999% pure hydrogen. Prior to loading into the reactor, the substrates were solvent cleaned and then etched in a solution of 15:3:1 $\text{H}_2\text{O}:\text{NH}_4\text{OH}:\text{H}_2\text{O}_2$, followed by rinsing in deionized water. Before initiating the growth process, the GaAs substrates were thermally cleaned at 540°C in 100 Torr of hydrogen until a sharp (2×4) reconstruction characteristic of a clean GaAs surface was observed.⁹ This thermal cleaning was completed in ≈ 10 min.

Two types of growth processes were studied in this work, continuous and interrupted. First, we grew films of ZnSe onto the GaAs substrates heated to 500°C using a continuous supply of both Et_2Zn and Et_2Se in a 1:4 ratio. In Fig. 1, diffraction data taken during growth along the (110) direction after ≈ 5 min of growth are presented. These data were taken while the incident x-ray beam was totally reflected from the surface and are sensitive to the structure of the top 25 Å of the film. Additional measurements demonstrated that this surface had a $p(2 \times 1)$ reconstruction which is similar to the reconstructions present during MBE growth of ZnSe.¹⁰ This structure was stable under a variety of Se/Zn ratios and growth temperatures.

A nonlinear least-squares analysis of the surface structure using five symmetry-inequivalent reflections yielded the dimer model (with a $\chi^2=1.6$) presented in the inset

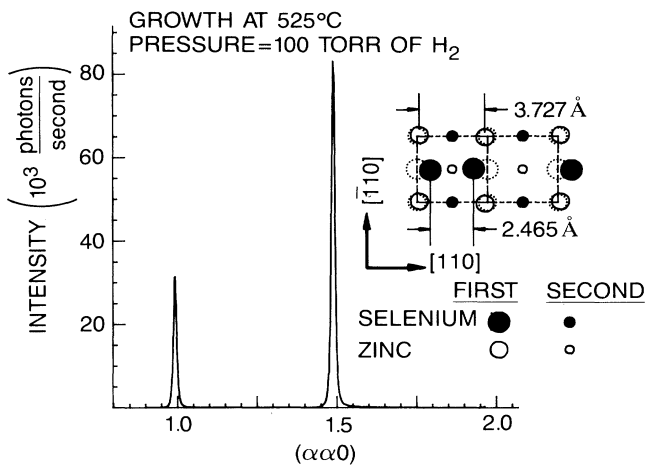


FIG. 1. An x-ray diffraction pattern from a growing ZnSe (001) surface. Even though growth is proceeding at high temperature and near atmospheric pressure, the diffraction peaks are very sharp and the backgrounds are extremely low. Inset: Real-space diagram of a dimer model consistent with these data. The Se atoms are displaced from their unreconstructed positions (dotted circles) by $(0.77 \text{ \AA}, -0.04 \text{ \AA})$ and $(-0.77 \text{ \AA}, 0.04 \text{ \AA})$; the Zn atoms are displaced by $(0.14 \text{ \AA}, 0.07 \text{ \AA})$ and $(-0.14 \text{ \AA}, -0.07 \text{ \AA})$.

in Fig. 1. In this analysis, we have assumed that the surface is terminated with Se atoms because we are growing with excess selenium. With this model, the Se atoms each form two bonds with the underlying Zn layer and dimerize with an adjacent Se atom. This structure is also similar to that of the $\text{Si}(001)2 \times 1$ reconstructed surface.¹¹ The presence of this reconstruction during growth and not the corresponding reconstruction from a Zn-terminated surface suggests that this growth is limited by nucleation of Zn layers.

Information about long-range order and film perfection can also be deduced by line-shape analysis. Figure 2(a) shows the same diffraction data plotted on a logarithmic scale and fitted with three Lorentzians, one for each of the diffraction peaks. While this fit appears quite good, the slight asymmetry of the peaks results in $\chi^2 \approx 6.7$. From this fitting procedure we obtain a width of 0.016 \AA^{-1} for the $(\frac{3}{2}, \frac{3}{2}, 0.05)$ reflection implying surface correlation lengths of 60 Å. Since this correlation length was measured during growth of a monolayer

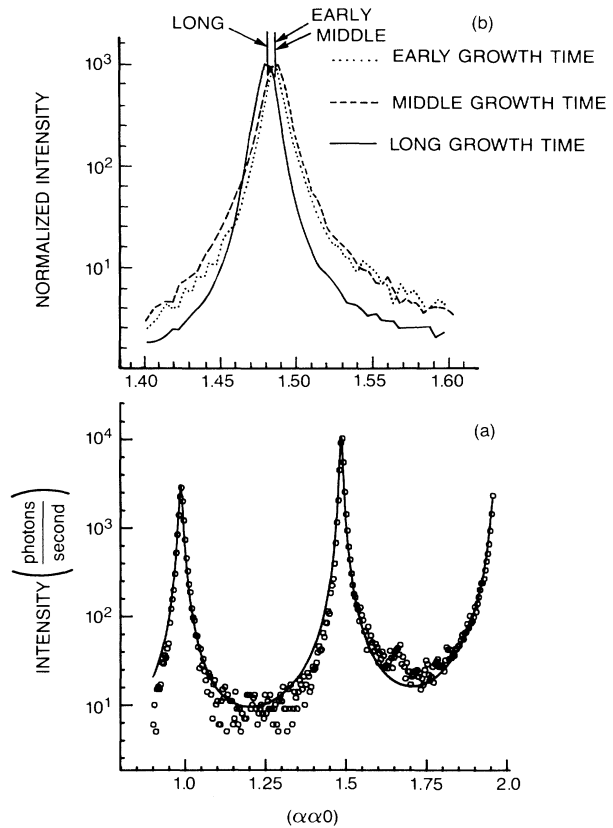


FIG. 2. (a) The logarithm of the data shown linearly in Fig. 1 plotted along with a Lorentzian fit. The width of the Lorentzian is 0.016 \AA^{-1} FWHM corresponding to correlation lengths on the surface of 60 Å. (b) The $(\frac{3}{2}, \frac{3}{2}, 0.05)$ reflection in more detail for several different growth times. Note the change in peak position and the change in line shape as a thicker film is grown.

per second at 525 °C, it indirectly measures the kinetics of nucleation. That is, the minimum distance between Zn-terminated regions must be at least the correlation length of the Se-terminated reconstruction.

Also shown in Fig. 2(b) is a series of $(\frac{3}{2}, \frac{3}{2}, 0.05)$ diffraction peaks taken from the same sample after different amounts of growth. There is a clear shift in the peak position towards lower momentum transfer (larger d spacing) after a certain amount of growth. At the same time, the line shape changes from being predominantly Lorentzian to predominantly Gaussian. [Fitting the $(\frac{3}{2}, \frac{3}{2}, 0.05)$ peak with a sum of Lorentzian and Gaussian line shapes results in > 85% Lorentzian for the first two curves and 40% Lorentzian for the final curve.] This change in both peak position and line shape reflects the evolution of the grown film from a thin strained epitaxial layer to a bulk ZnSe film relaxed by the introduction of misfit dislocations. The film shown in Fig. 2 was grown with a variety of conditions and OM ratios and the resulting structure seems to be dependent only on film thickness. Because the growth rate was varied, assignment of a specific thickness to each curve is difficult.

The nature of the growing film can also be probed by looking at diffraction profiles perpendicular to the surface. Figure 3 shows the diffracted intensity between the (110) and the $(1, 1, \frac{4}{5})$ [normal to the (001) surface]. The diffracted intensity from this clean, reconstructed surface grows uniformly towards the (111) bulk allowed reflection and is representative of a surface truncation rod.¹² During growth of a ZnSe film on this surface, the same diffraction scan reveals a much different structure which is composed of three components. The dominant feature is a flat spectrum from a two-dimensional reconstruction. This flat spectrum is modified near $l=0$ by refractive-index effects which result in a small peak.

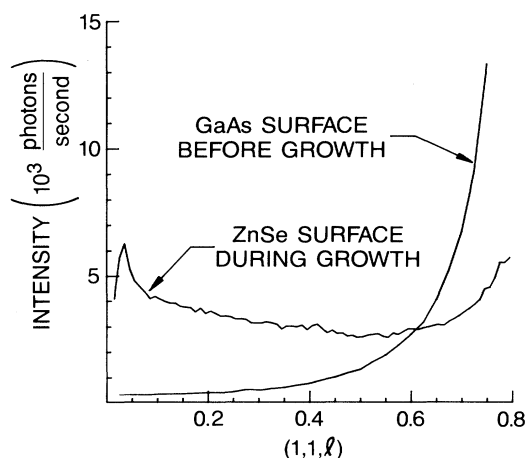


FIG. 3. X-ray diffraction data taken normal to the surface and through the GaAs (110) and the ZnSe (110) reflection. Note the dramatic difference between the GaAs surface prior to growth and the ZnSe surface during growth.

(This effect, which is well understood from classical electromagnetic theory, is also present from the GaAs surface when data are collected on a finer mesh.) Finally, the data rise at high l due to the ZnSe (111) reflection. This profile demonstrates the two-dimensional nature of the growing interface and its associated reconstruction. This diffuse rod in reciprocal space is similar in nature and origin to "streaky" RHEED patterns often found in MBE growth.

The final set of experiments discussed in this paper investigated the equilibration of surface structure with changes in growth conditions. One such experiment is x-ray reflectivity measurements during alternate-source epitaxy (ASE). During ASE, the surface is saturated with one species, allowed to relax, saturated with the other species, and allowed to relax.¹³ This process is repeated numerous times to build up an epitaxial film. Figure 4 shows the specular reflectivity at a momentum transfer of $k = (4\pi/\lambda) \sin(\theta) = 0.504 \text{ \AA}^{-1}$ from a film being grown by ASE at 450 °C. Clearly, there are dramatic changes in reflectivity directly correlated with changes in organometallic flows. The inset in Fig. 4 shows an enlarged view of one cycle of growth along with a measure of the gas switching time. (The measure of the gas switching time was made by observing the difference in N_2 and H_2 diffuse scattering.) While the gas switching occurs in ≈ 1 sec, the surface reflectivity requires ≈ 40 sec to respond. Thus, the dynamics of gas/surface equi-

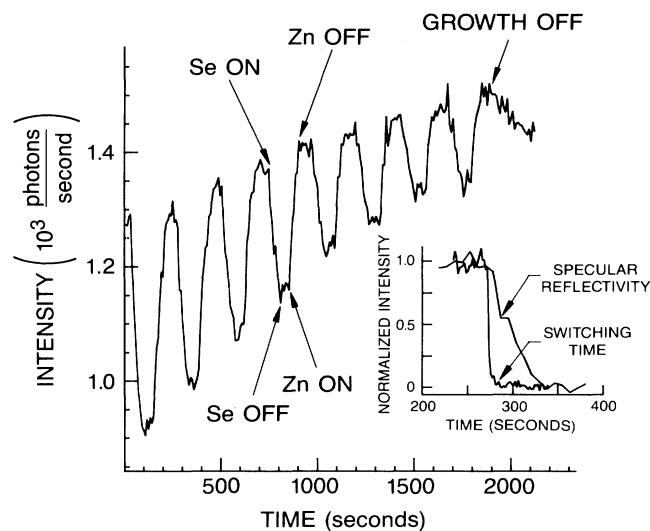


FIG. 4. X-ray specular reflectivity measurements made during OMVPE growth at 450 °C. The growth mode used, alternate-source epitaxy, consisted of (1) turning on the Et_2Se source for 1 min, (2) turning off the reactive-gas flow for 1 min, (3) turning on the Et_2Zn source for 1 min, and (4) turning off the reactive-gas flow for 1 min. This 4-min cycle was then repeated. Inset: An expanded view of one cycle and, superimposed, a direct measurement of the gas-flow switching time.

bration are probed by this measurement.

It is tempting to ascribe these fluctuations to alternate growth of Se and Zn layers in the same manner as is done with RHEED oscillation data. However, the data seem best described by saturation of the surface with partially decomposed Et_2Se , thus reducing the interface sharpness and reflectivity. During the Et_2Zn flow, the Et_2Se reacts with Zn atoms, restoring a sharp interface and increasing the specular reflectivity. This model is supported by kinetic measurements which indicate that Et_2Se does not decompose at these lower temperatures and that Et_2Zn does.¹⁴ Measurements at higher temperatures yield curves similar in appearance but with the phase changed. That is, instead of initially falling with introduction of the Et_2Se , the reflectivity initially increases. This behavior appears to support the latter interpretation of these data but a definitive explanation requires additional measurements.

With these initial experiments, we have demonstrated the power of x-ray diffraction techniques for the *in situ* analysis of chemical-vapor deposition and, in particular, organometallic-vapor-phase epitaxy. Our current experiments have demonstrated excellent surface sensitivity, high signal rates, and low backgrounds. This powerful tool can be used to study a wide range of challenging systems. Starting with ZnSe, the detailed nature of growth transients can be elucidated along with their relationship to reflected beam intensities; the growth mechanism as a function of growth parameters such as temperature, pressure, and source compounds can be studied. In addition, by growing $\text{ZnSe}_x\text{S}_{1-x}$ the lattice mismatch with GaAs can be systematically varied. The *in situ* measurement of strain in the overlayer and its subsequent release by formation of misfit dislocations will give valuable insight into the kinetics of lattice relaxation in mismatched systems. Finally, it is straightforward to extend this technique to other systems, an important example of which would be the study of the initial stages of growth of GaAs on silicon, where the structural details of the interface apparently control the resulting film properties.¹⁵

In summary, coupling the brightest x-ray source with proven x-ray-scattering techniques, we have developed a powerful tool for *in situ* analysis of CVD systems. We expect the understanding gained by the application of this tool will lead to a deeper understanding of these complex processes and to the subsequent development of new CVD techniques and methods.

The authors gratefully acknowledge the help of the large number of SSRL personnel who worked very hard to make these experiments happen. They include J. Cerino, D. Day, H. Przybylski, R. Silvers, C. Troxel, and T. Troxel. In addition, several AT&T Bell Labs colleagues have contributed through discussions and support, including L. J. Norton, R. D. Feldman, A. Ourmazd, C. V. Shank, and A. M. Glass. One of us (S.B.) was supported by the Department of Energy, Office of Basic Energy Sciences. Work was done at the Stanford Synchrotron Radiation Laboratory which is supported by the Department of Energy, Division of Chemical Sciences.

¹G. B. Stringfellow, *Organometallic Vapor Phase Epitaxy: Theory and Practice* (Academic, Boston, 1989).

²P. W. Lee, T. R. Olmstead, D. R. McKenna, and K. F. Jensen, *J. Cryst. Growth* **93**, 134 (1988); C. A. Larsen, N. I. Buchan, and G. B. Stringfellow, *Appl. Phys. Lett.* **52**, 480 (1988).

³J. E. Butler, N. Bottka, R. S. Sillmon, and D. K. Gaskill, *J. Cryst. Growth* **77**, 163 (1986).

⁴D. E. Aspnes, E. Colas, A. A. Studna, R. Bhat, M. A. Koza, and V. G. Keramidis, *Phys. Rev. Lett.* **61**, 2782 (1988).

⁵P. Eisenberger and W. C. Marra, *Phys. Rev. Lett.* **46**, 1081 (1981).

⁶P. H. Fuoss, K. S. Liang, and P. Eisenberger, in *Synchrotron Radiation Research: Advances in Surface Science*, edited by R. Z. Bachrach (Plenum, New York, to be published).

⁷S. Brennan and P. Eisenberger, *Nucl. Instrum. Methods Phys. Res., Sect. A* **222**, 164 (1984).

⁸S. Brennan, P. H. Fuoss, J. L. Kahn, and D. W. Kisker, in *Proceedings of the 1989 Synchrotron Radiation Instrumentation Conference*, Berkeley, California (to be published).

⁹P. H. Fuoss, D. W. Kisker, G. Renaud, K. L. Tokuda, S. Brennan, and J. L. Kahn, SSRL Activity Report, 1989 (unpublished); D. W. Kisker, P. H. Fuoss, G. Renaud, K. L. Tokuda, S. Brennan, and J. L. Kahn (to be published).

¹⁰J. M. Depuydt, H. Cheng, J. E. Potts, T. L. Smith, and S. K. Mohapatra, *J. Appl. Phys.* **62**, 4756 (1987).

¹¹W. S. Yang, F. Jona, and P. M. Marcus, *Phys. Rev. B* **28**, 2049 (1983).

¹²S. R. Andrews and R. A. Cowley, *J. Phys. C* **18**, 6427 (1985); I. K. Robinson, *Phys. Rev. B* **33**, 3830 (1986).

¹³S. P. DenBaars, C. A. Beyler, A. Hariz, and P. D. Dapkus, *Appl. Phys. Lett.* **51**, 1530 (1987).

¹⁴H. Mitsuhashi, I. Mitsuishi, and H. Kukimoto, *J. Cryst. Growth* **77**, 219 (1986).

¹⁵R. M. Lum, J. K. Klingert, B. A. Davidson, and M. G. Lamont, *Appl. Phys. Lett.* **51**, 36 (1987).